applied sciences

MDPI

Article

The Combination of Low-Temperature Plasma and *Tripterygium wilfordii Hook F* on Ameliorating Imiquimod-Induced Psoriasiform Dermatitis in Mice

Song Zhang [1], Baihan Chen [2], Dawei Liu [2,3,*] and Hongxiang Chen [1,4,*]

1 Department of Dermatology, Union Hospital, Tongji Medical College, Huazhong University of Science and Technology, Wuhan 430022, China; zhangsong767@hust.edu.cn
2 State Key Lab of Advanced Electromagnetic Engineering and Technology, School of Electrical and Electronic Engineering, Huazhong University of Science and Technology, Wuhan 430074, China; m201971504@hust.edu.cn
3 Wuhan National High Magnetic Field Center, Wuhan 430074, China
4 Department of Dermatology, Huazhong University of Science and Technology Union Shenzhen Hospital, Shenzhen 518052, China
* Correspondence: liudw@hust.edu.cn (D.L.); hongxiangchen@hotmail.com (H.C.)

Abstract: Improving the transdermal delivery efficiency of medicine is a crucial measure to improve the treatment efficiency of psoriasis. This paper developed a low-cost, highly active, and large-action-area low-temperature plasma (LTP) jet array. The two components of plasma—the high concentration of reactive oxygen and nitrogen species and the strong electric field—easily changed the structural integrity of the stratum corneum, which enhanced the transdermal delivery of the medicine. *Tripterygium wilfordii Hook F* (TwHF) is a medicine used to treat autoimmune and inflammatory conditions. The enhanced transdermal delivery of TwHF significantly alleviated the severed psoriasiform dermatitis induced by the imiquimod. Unlike the TwHF treatment alone, the LTP + TwHF treatment was more efficient at suppressing epidermal thickening and inhibiting systemic inflammation without noticeable side effects. LTP + TwHF treatment provides a potential new solution for psoriasis treatment.

Keywords: plasma; psoriasiform dermatitis; transdermal delivery; *Tripterygium wilfordii hook F*

Citation: Zhang, S.; Chen, B.; Liu, D.; Chen, H. The Combination of Low-Temperature Plasma and *Tripterygium wilfordii Hook F* on Ameliorating Imiquimod-Induced Psoriasiform Dermatitis in Mice. *Appl. Sci.* **2022**, *12*, 356. https://doi.org/10.3390/app12010356

Academic Editor: Emilio Martines

Received: 14 October 2021
Accepted: 20 December 2021
Published: 30 December 2021

1. Introduction

Psoriasis is a chronic immune-mediated inflammatory skin disease associated with high prevalence, disfigurement, and comorbid diseases [1–5]. Psoriatic lesions usually manifest as erythematous-thickened plaques with silvery scales, whose key pathogenic events include keratinocyte hyperproliferation, marked inflammatory infiltration, and pathological angiogenesis [6,7]. Although available treatments can relieve many symptoms, there is still currently no cure [8].

Given its combination of a high concentration of reactive oxygen and nitrogen species (RONS), energetic electrons, and a strong electric field, low-temperature plasma (LTP) has received much attention for applications to wound healing and in the treatment of inflammatory skin diseases [9–14]. The ability to maximize and control the penetration depth of LTP in the skin can effectively improve the therapeutic efficiency of LTP in skin disease treatment, which also means the transdermal effect of LTP provides the possibility of improving the efficiency of traditional medical treatment.

Tripterygium wilfordii Hook F (TwHF) has significant anti-inflammatory and immunomodulatory effects [15]. It has successfully treated various clinical immune abnormalities and has achieved fairly reliable curative results [16]. TwHF has a specific cytotoxic effect and can control abnormal cell proliferation in psoriasis [17].

In this paper, we developed a safe, low-cost, and effective LTP jet array. The active plasma, with its large action area, efficiently disrupts the stratum corneum structure. Therefore, the transdermal delivery of imiquimod (IMQ) and TwHF was enhanced. The improved transdermal delivery of TwHF alleviated the more severed psoriasiform dermatitis that was induced by the enhanced transdermal delivery of IMQ. Unlike TwHF treatment alone, the LTP + TwHF treatment showed even lower cumulative scores, epidermal thickening, inflammatory cell infiltration, and inflammatory cytokines released in the IMQ-induced psoriasis-like mouse model. The LTP + TwHF treatment also efficiently reduced the enlargement of the spleen [18,19].

2. Experiment Setup and Methods

2.1. Reagents

Tripterygium wilfordii Hook F (TwHF) (YiCaoTang Co. Ltd., Shanghai, China) was dissolved in distilled water (BKMAM, B-ZLS500) to make the stock solutions (c = 55.8 mmol/L).

2.2. IMQ-Induced Psoriatic-Like Mouse Model

The BALB/c mice used in the experiment were bought from HFK Bioscience (Beijing Co., Ltd., Beijng, China). These mice were bred in the animal facility under specific pathogen-free conditions for 10 days before the experiment. These mice were also weight and age matched. Animal experiments were performed in the USUHS laboratory animal facility. The protocol used in this study was approved by the USUHS Institutional Animal Care and Use Committee [20].

The dorsal hair of mice (8–10 weeks of age) was removed across a surface area of ~4–5 cm^2 [1]. Next, 5% imiquimod (IMQ) cream (Mingxin Lidi Laboratory, Shanghai, China) was applied daily (at 07:00 AM) at a topical dose of 62.5 mg for 7 days to establish an IMQ-induced psoriasis mouse model [20]. The BALB/c mice were randomly divided into the following groups: control group; IMQ-treated group (topical dose with 62.5 mg of 5% IMQ cream alone, at 07:00 every day); LTP-treated group (LTP treatments for 10 min/day, at 13:00 every day); TWHF group (1 mg/cm^2/day, at 19:00 every day); LTP + TWHF group (LTP treatments for 10 min followed by TWHF treatment, at 13:00 every day). Each group had five mice, and seven consecutive days of administration or plasma treatment was necessary for all mice. All mice were euthanized 24 h after the last treatment via cervical dislocation and the dorsal skins were collected.

Another group of mice was used to study the penetration effect of LTP on mouse skin. A depilatory paste removed the mice's hairs, and the mice were killed via cervical dislocation after 24 h. A pair of small scissors was used to cut out the dorsal skin. Then, the isolated skin's subcutaneous tissue was scraped off cleanly with a surgical knife and washed with phosphate buffer saline (PBS) [1]. The isolated skin was covered with bibulous paper to remove the excess water and then immediately treated with the LTP jet array. Because the stratum corneum (SC) is an important skin barrier, the treatment position on the isolated skin was fixed without any movement for 5–10 min to study the effect of the plasma on the structural integrity of the SC.

2.3. Measurement of Skin Inflammation Severity, Immunohistochemistry and Cytokine Detection via Quantitative Real-Time PCR

The Psoriasis Area and Severity Index (PASI) includes measurements of skin thickness, erythema, and scale. The same measurements were carried out in our previous study [20]. All mice were evaluated as IMQ was administrated for seven consecutive days. The mouse skin's thickness was measured using a micrometer and averaged five times. In order to measure the epidermal thickness and cellular accumulation, surgical specimens of dorsal skin tissues were paraffin-embedded for H&E staining [20]. Paraffin-embedded tissues sections (4 mm) were stained with hematoxylin (Beyotime, Haimen, China) for 40 s and with eosin (Beyotime, China) for 30 s [20]. An OLYMPUS light microscope was used to

measure the tissue sections. Photoshop in three separated fields of view was used to measure the mouse epidermis's thickness.

Skin tissues were fixed with 4% paraformaldehyde for 2 days and embedded with paraffin. Afterward, samples were cut into 4 mm thick slides. For immunohistochemistry, sections were sequentially incubated with the primary antibody anti-CD3 (1:100, Abcam) and the secondary antibody HRP anti-rabbit IgG (Maxim), and then the color was developed with diaminobenzidine. Image J software was used to measure the region where CD3+ cells accumulated for quantitative analyses, and accumulation was expressed as the percentage of positive cells. Twenty-four hours after the last treatment, the mice were euthanized via cervical dislocation, and the spleens, as well as the axillary and inguinal lymph nodes, were separated and placed in pre-cooled PBS. We removed the attached connective tissue of the spleens, and the axillary and inguinal lymph nodes, then put a 0.1 cm^3 tissue into 1 mL of saline. We carefully cut the tissue, and ground it thoroughly in a homogenizer to obtain the tissue suspension. The prepared 10% homogenate was centrifuged at 4 degrees at 3000 rpm for 15 min, and the precipitate was taken for RT-PCR detection. The reverse transcription and real-time PCR analysis were measured by the same method used in ref. [20]. The primers used in this experiment were: *Il1* mice F: GCAACT GTTCCTGAACTCAACT R: ATCTTTTGGGGTCCGTCCAACT *Il4* mice F: TCGTCTGTAGGGCTTCCAAGGTGCT R: GTGGACTTGGACTCATTCATGGTGC Il6 mice F: GACAAAGCCAGAGTCCTTCAGAGAGA R: GGTCTTGGTCCTTAGCCACTCCTT *Il17a* mice F: CCTCAGACTACCTCAACCGTTCC R: AGGCTCCCTCTTCAGGACCAG GAPDH mice F: AACTTTGGCATTGTGGAAGG R: ACACATTGGGGGTAGGAACA.

2.4. Statistical Analyses

Statistical comparisons between two groups were performed by using a Student's t test. GraphPad Software Prism 6.0 was used for statistical analysis. p values < 0.05 were considered to be significant [20].

2.5. LTP Jet Array System

Figure 1 shows the LTP jet array treating imiquimod-induced psoriasiform dermatitis in mice. The inserted picture in Figure 2 shows that the LTP jet array had a treatment area with a diameter of 1.5 cm. A uniform plasma plume was generated on the mouse back and on an irregular edible gelatin surface by the LTP jet array, which indicates that the LTP jet array can handle multiple targets with different structures. The plasma jet array consisted of three quartz glass tubes (8 mm outer diameter, 5 mm inner diameter) (Figure 2) [18]. Two coils of copper wire were wrapped around each tube. The narrower at the top is the anode, and the wider at the bottom is the ground electrode. The working gas (argon + O_2) was fed into the tubes. Three working gas admixture ratios were set as argon (6 slm), argon (6 slm) + O_2 (6 sccm, 0.1% of the argon flow rate), and argon (6 slm) + O_2 (60 sccm, 1%). A homemade 24 kHz AC power supply drove the discharge. The total cost of the LTP jet array was less than USD 200. A digital camera (Nikon D800) took plasma images from the side of the plasma jet. A broadband optical emission spectrum (from 200 to 1000 nm) was measured with an optical spectrometer (Ocean optics USB 2000, 4 nm resolution). A thermometer (Yufei 888, 0–50 °C ± 0.1 °C) measured the gas temperature of the plasma. The O_3 concentration of the plasma was measured via UV absorption spectroscopy [19]. The NO concentration was measured with a multi-gas detector (RAE Systems, PGM-7800).

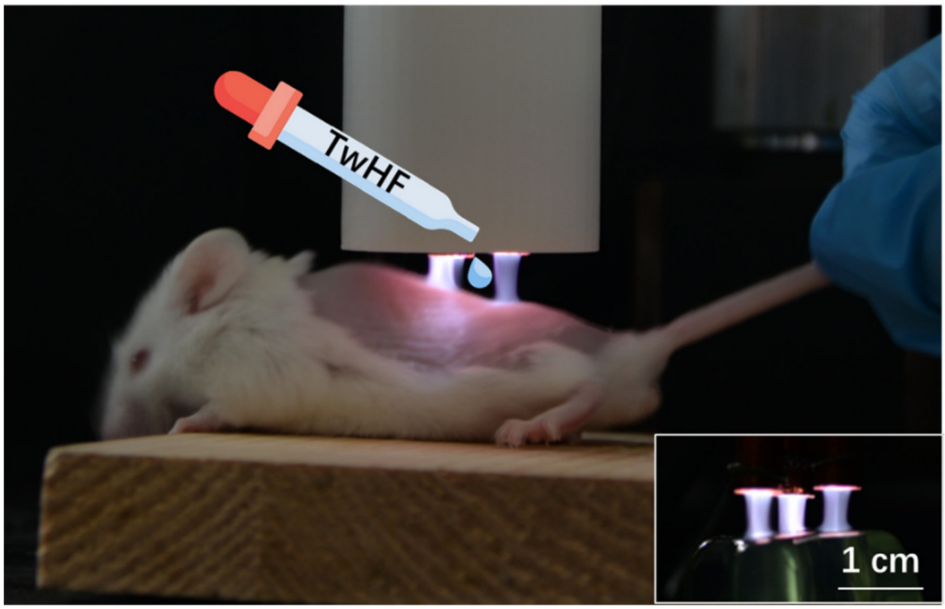

Figure 1. Photo of the combined treatment of imiquimod-induced psoriasiform dermatitis in mice by the LTP jet array and with TwHF.

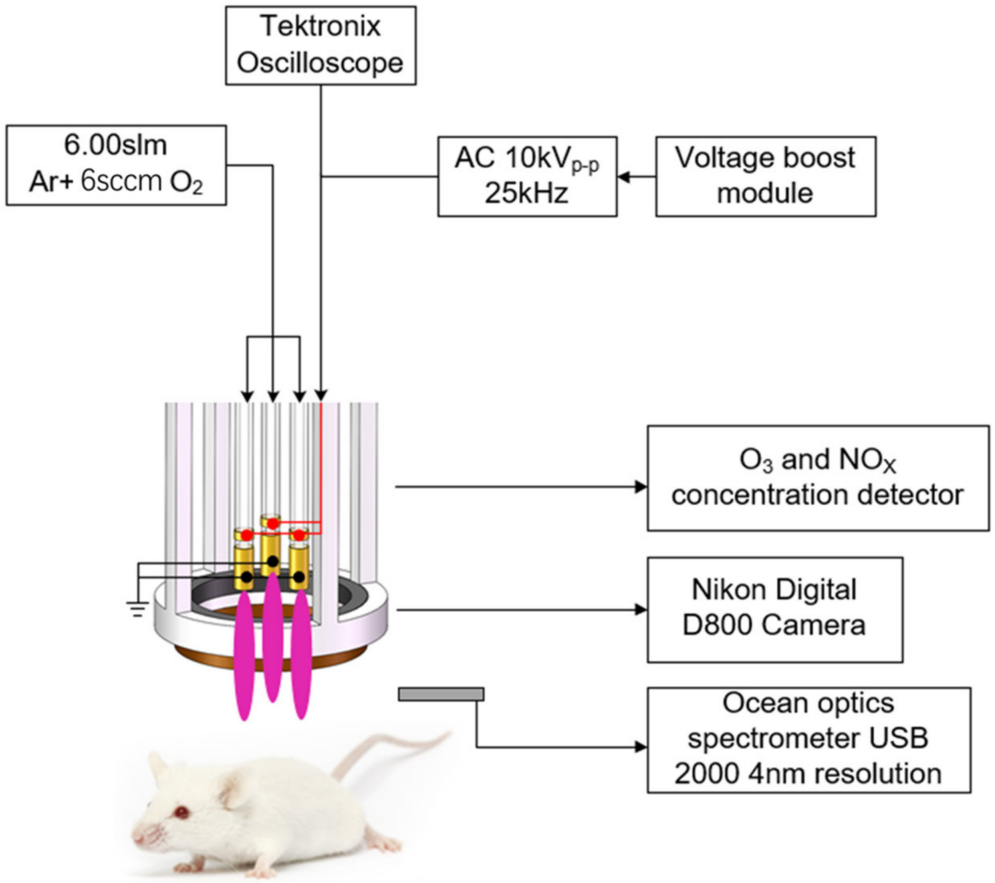

Figure 2. Schematic illustration of the LTP jet array. Experimental setups for optical diagnostics, gas temperatures, and long-lived reactive species. The inserted picture shows the LTP jet array with a diameter of 1.5 cm generated on an edible gelatin.

3. Results and Analysis

3.1. Characteristics of LTP Jet Array

Figure 3a shows the current and voltage characteristics of the LTP jet array. The peak value of the applied voltage was 9 kV. The current peaks shown in Figure 3a suggest that the discharge mainly occurred at the rising phase of the positive and negative half cycle. The length of the plasma plume of the LTP jet array with the working gas of argon alone was about 2 cm, and it decreased to 1.7 cm and 0.9 cm for the working gas with an O_2 percentage of 0.1% and 1%, respectively. The current peak was about 95 mA for the argon alone case, and it decreased by 50 mA as the O_2 percentage increased from 0 to 1%. The plasma plume of the LTP jet array can be touched by hand directly. The gas temperature of the plasma plume measured by the thermometer was 25 ± 2 °C. The difference in the gas temperature of the LTP jet array between the different O_2 percentages was negligible.

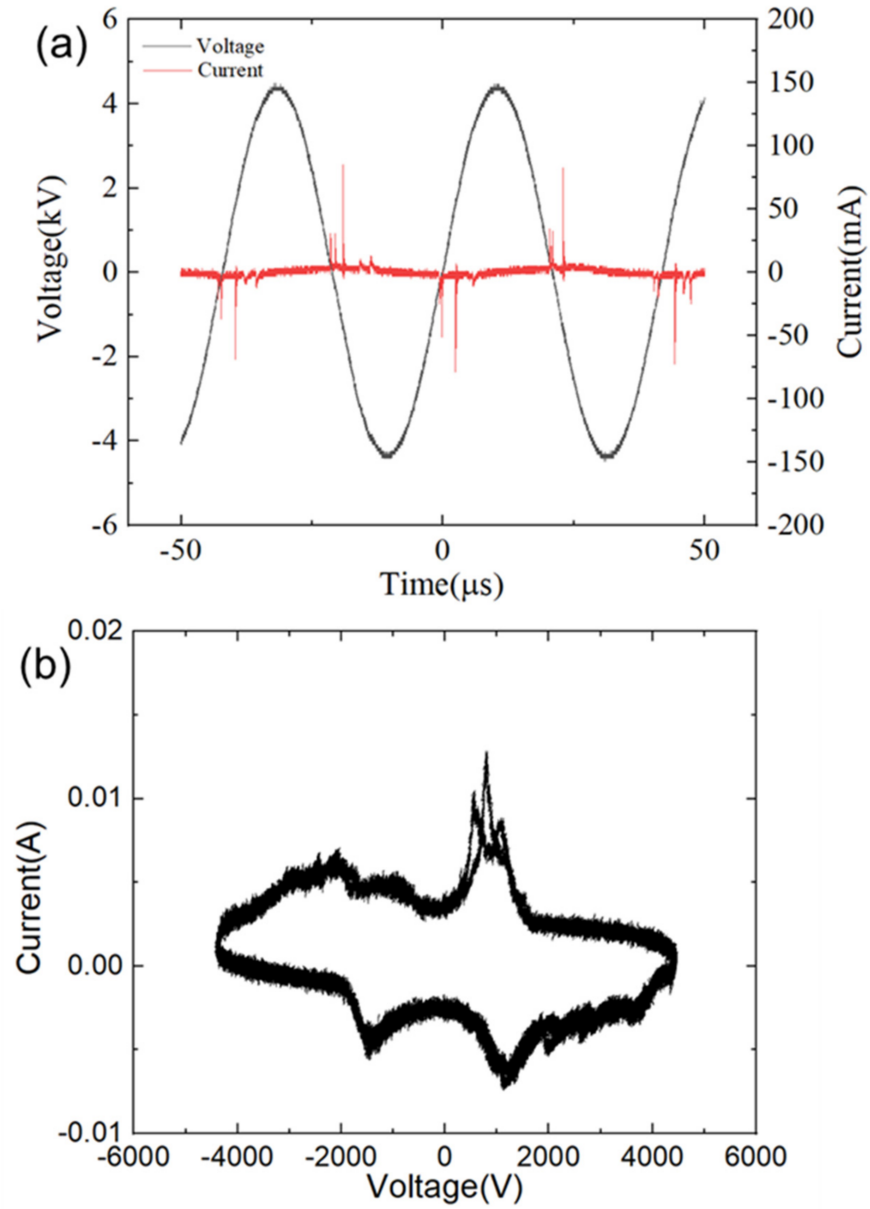

Figure 3. (**a**) Current and voltage characteristics of the LPT jet array (with the working gas of argon alone). Because the difference of the CVC between argon, argon + 0.1% O_2, argon + 1% O_2 was negligible, only one group of CVC is plotted. (**b**) The Lissajous figure corresponding to (**a**) was used to calculate the power of the LPT jet array.

The power of the LTP jet array was calculated using Equation (1) based on the Lissajous figure shown in Figure 3b [21]:

$$P = \frac{1}{T}\int_0^T UIdt = \frac{C_M}{T}\int_0^T U\frac{dU_M}{dt}dt = fC_M\int_0^T UdU_M = fC_MS \quad (1)$$

In Equation (1), P, U, I, f, C_M, and S are the power, voltage, current, discharge frequency, capacitor of the LTP jet array, and the area of the closed voltage–current curve in the Lissajous figure, respectively. The capacitance of the plasma jet array measured using the impedance analyzer was 9.756 pF. The power of the argon, argon + 0.1% O_2, argon + 1% O_2 cases was 1.88 W, 1.64 W, and 1.32 W, respectively.

The addition of O_2 into the working gas also affected the reactivity of the LTP jet array significantly. The optical emission spectrum (OES) shown in Figure 4 indicated that the OES of atomic oxygen at O ($3s^5S$-$3p^5P$) 777 nm and O ($3p^54p$-$3p^56s$) 844 nm increased by about 40% as the O_2 ratio increased from 0 to 0.1% and decreased by 63.3% as the O_2 percentage increased from 0.1% to 1% [22,23]. Energetic electrons with electron energy >10 eV are needed to generate the excited atomic oxygen corresponding to the OES at 777 nm and 844 nm [22,24–26]; therefore, the concentration of atomic oxygen in the ground state was much higher than that in the excited state [27,28]. For example, the absolutely calibrated TALIF measurement of atomic oxygen in the grounded state in the effluent of the similar argon plasma jet indicated that the atomic oxygen density was in the order of $10^{15}/cm^3$, and that it decreased with the distance to the nozzle by up to an order of magnitude [29]. The increasing at first and decreasing afterward trend of the OES was also consistent with the evolution of atomic oxygen in the ground state as a function of the O_2 admixture ratio measured by TALIF [10,30]. More electrons consumed by attachments to oxygen, $e + O_2 \Rightarrow O_2^-$, results in the decreasing discharge intensity and decreasing reactivity as the O_2 admixture ratio increased from 0.1% to 1% [31].

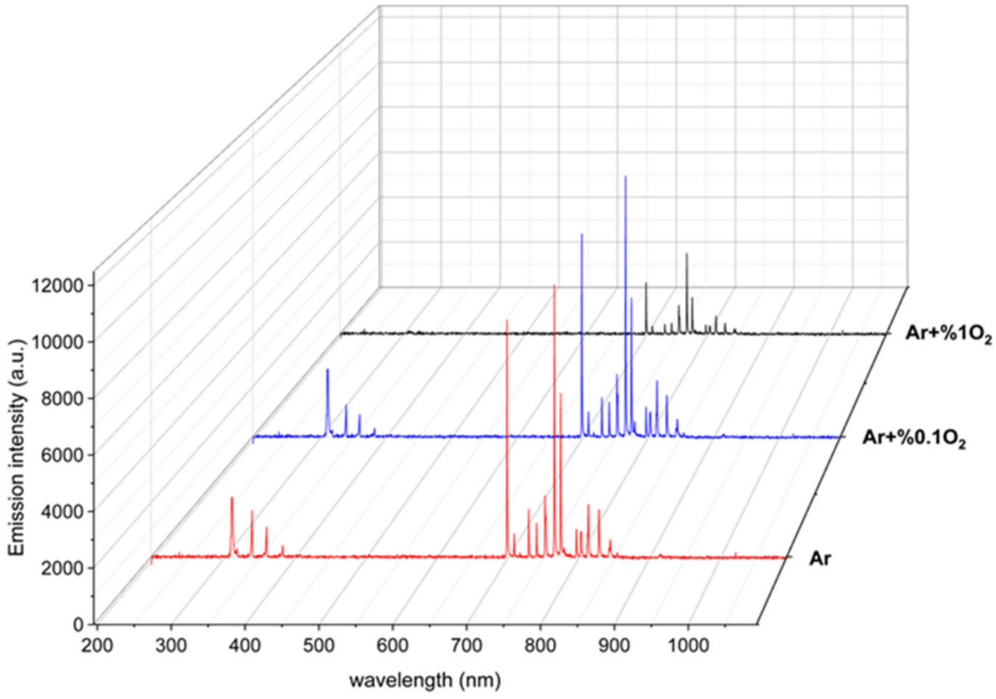

Figure 4. The optical emission spectroscopy of the LTP jet array with the working gas of argon, argon + 0.1% O_2, argon + 1% O_2.

Figure 5 shows O_3 and NO density as a function of the O_2 admixture ratio. As the O_2 admixture ratio increased from 0 to 1%, O_3 density increased from 18 ppm to 43 ppm (0.1% O_2) and 25 ppm (1% O_2). The peak concentration of NO was 6 ppm when the

O_2 admixture ratio was 0.1%. The further increasing of the O_2 admixture ratio to 1% decreased NO concentration below the detection limit of the measurement device. Besides the decreasing discharge intensity, the transition of NO to NO_2 through the reaction of NO + O => NO_2 [9,10] was also the main reason for the decreasing NO concentration with the increasing O_2 admixture ratio.

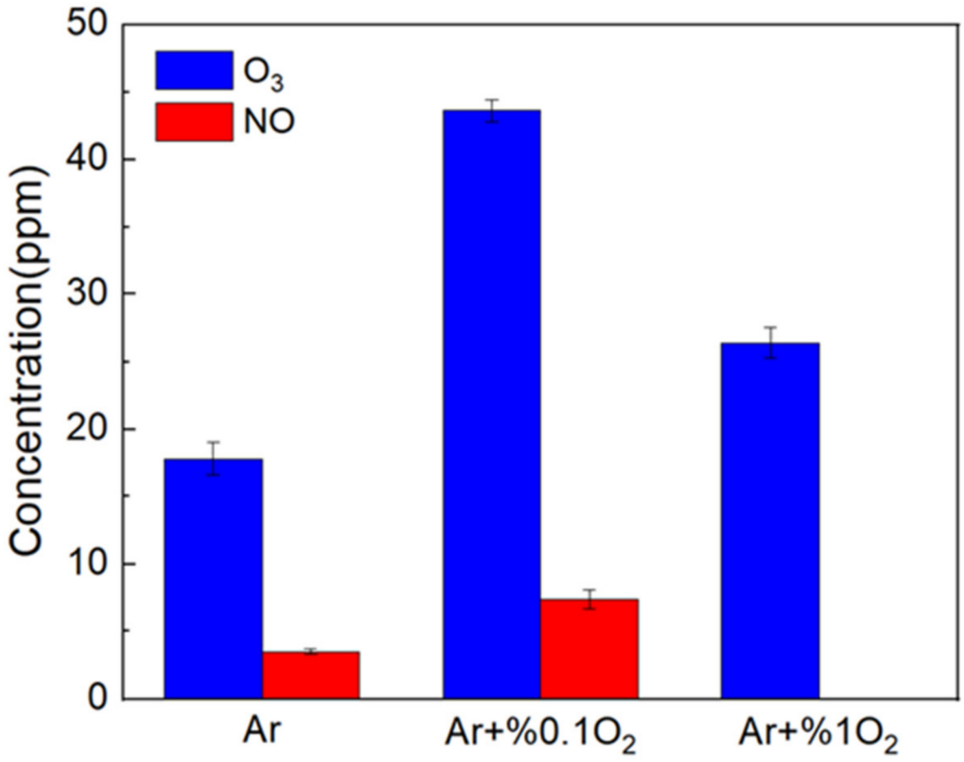

Figure 5. Concentration of O_3 and NO for the LTP jet array with the working gas of argon, argon + 0.1% O_2, argon + 1% O_2.

As the main RONS generated by plasma, O, O_3, and NO can increase skin permeability through a complex series of reactions. The increase in the number of C–O or C=O bonds after the LTP treatment of the skin layer also confirmed the incorporation of oxygen to the stratum corneum lipids [32]. The reactions between O, O_3, and *a*-linolenic acid as a representative of fatty acid can create a double bond, incorporate alcohols or aldehyde groups, and increase the hydrophilic properties of fatty acids and change the lipid composition of skin, and thus eventually increases skin permeability [33]. Moreover, NO_x species can acidify the lipids stripped from the stratum corneum, which also affects the skin permeability significantly [34,35], although the pH of the skin can return to the initial value within 30 min after plasma treatment [36]. Therefore, the LTP jet array with the working gas of argon + 0.1% O_2 was used to treat IMQ-induced psoriasiform dermatitis with TwHF.

LTP has an essential effect on the structural integrity of the stratum corneum (SC) layer. Figure 6 shows that the 5 min LTP treatment (the processing point remained fixed) caused damages to the SC layer of the isolated skin (blue dashed rectangle), and that the 10 min LTP treatment obliterated the SC layer. Similar changes to the SC structures induced by LTP were also observed in the treatments that used other LTP sources [31,37,38]. Besides the lipid peroxidation caused by the RONS of plasma, the strong electric field and high-speed plasma particles also contributed to the structural change of the SC layer [3,4,10,11].

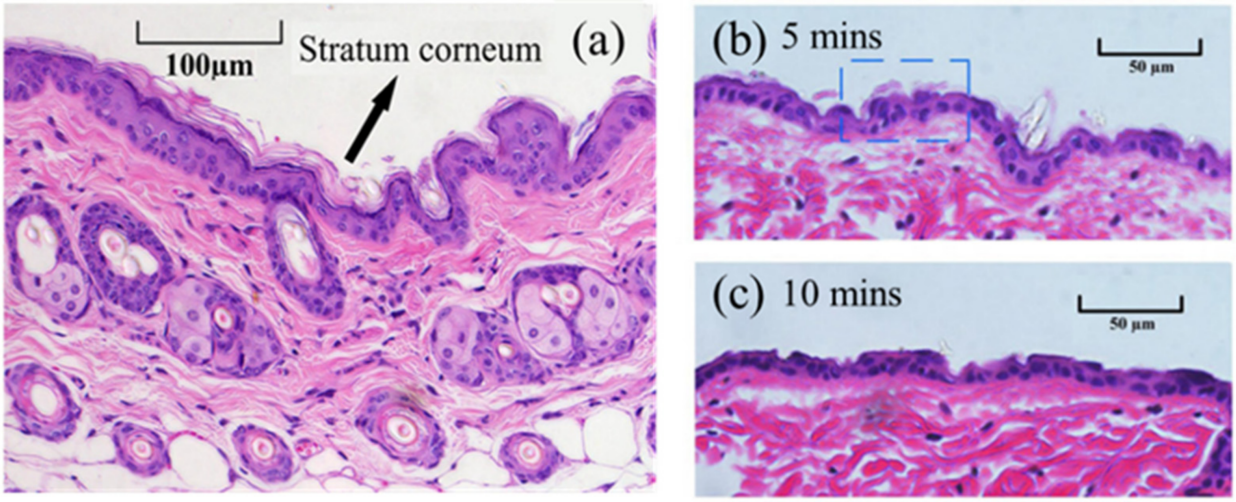

Figure 6. The HE (hematoxylin-eosin) staining of the mice skin before/after LTP treatment: (**a**) The HE staining of normal mice skin before plasma treatment. (**b**) The HE staining of normal skin after 5 min plasma treatment. The SC is damaged after Plasma treatment for 5 min. (**c**) SC is totally removed by the 10 min plasma treatment. Unlike the plasma scanning treatment for IMQ-induced psoriasis, the position of LTP treatment was fixed during SC damage treatment.

The scanning process of the LTP jet array on the IMQ-induced psoriatic region on the back of live mice in the following experiment decreased the contact time between the plasma and SC. The highly active plasma can still affect the structural integrity of the SC [39,40]. Even without noticeable structural change in the SC, the plasma-induced nitric oxides from keratinocytes can regulate the junctions between the cells and the extracellular matrix in the epidermal layer, which made the epidermal barrier permeable and facilitated the transdermal permeability of aniline blue [41].

3.2. Plasma + TwHF Treatment Ameliorated IMQ-Induced Psoriatic Skin Lesion

To confirm whether LTP + TwHF can efficiently ameliorate skin lesions in psoriasis, we used the IMQ-induced psoriasis-like mice with LTP treatment alone, TwHF treatment alone, and LTP + TwHF treatment. Mice in our animal experiment were randomly assigned into five groups: the Control, IMQ, LTP, TwHF, and LTP + TwHF groups. Figure 7 suggests that the dorsal skin treated with IMQ generated typical psoriasis-like inflammatory responses on the back, such as thickening, scaling, and erythema after 3 days, and lesions gradually increased with extended IMQ administration.

The LTP treatment aggravated the psoriatic lesions. The PASI score shown in Figure 7c suggests that the PASI scores of the LTP group were about 10% higher than that of the IMQ group. The main reason is the damage to the SC caused by plasma (as shown in Figure 6) and the subsequent enhancement in the transdermal delivery of IMQ.

TwHF notably alleviated the skin lesion throughout the treatment period (TwHF group in Figure 7b,c). The extracts from the root of TwHF inhibit the expression of proinflammatory cytokines, proinflammatory mediators, adhesion molecules, and matrix metalloproteinases. TwHF possesses potent anti-inflammatory and immunosuppressive properties in vitro and in different animal models in numerous preclinical studies [15,42,43].

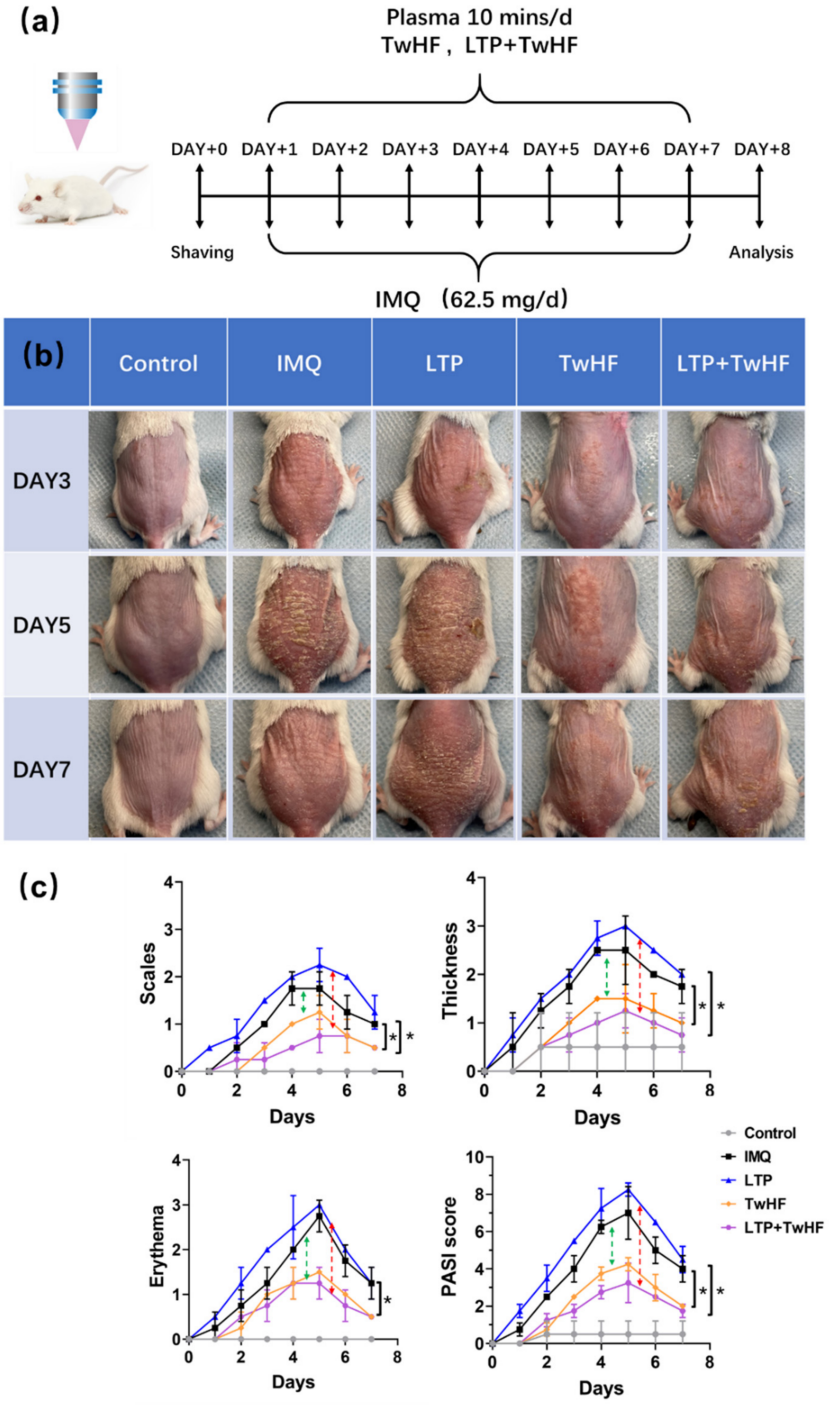

Figure 7. LTP + TwHF ameliorates psoriatic symptoms and skin inflammation in IMQ-induced psoriatic mice. (**a**) Flow chart of the experiment. (**b**) The back skin photos of mice were taken on the 3rd, 5th 7th day after IMQ painting. (**c**) PASI scores in all groups of mice were evaluated daily and the statistical difference between all groups was indicated. Data are expressed as mean ± SD (n = 5 mice/group, * $p < 0.05$). One representative of three separate experiments is shown while all results were similar among these three experiments. Because the LTP treatment enhanced the transdermal delivery of IMQ, the psoriasiform dermatitis became more serious after the LTP treatment. TwHF group only alleviated mild symptoms of the IMQ model. The comparison between the red dash line and green dash line suggests that the LTP + TwHF psoriasiform dermatitis is more efficient at suppressing epidermal thickening and inhibiting systemic inflammation.

LTP + TwHF also significantly alleviated the severity of the IMQ-induced psoriasis. The scores for erythema and thickness, along with the cumulative score of four groups are compared in Figure 7c. The decrease in the LTP group scores compared to the LTP + TwHF group is ~40% more than the decrease from the IMQ group to the TwHF group, which indicates that the LTP + TwHF treatment can reduce psoriasis symptoms more efficiently than TwHF treatment alone. The application of TwHF right after LTP treatment is expected to substantially enhance the transdermal delivery of TwHF. Therefore, the combination of LTP and TwHF realized the more efficient treatment on psoriatic lesions.

The H&E staining shown in Figure 8b captured the IMQ-induced psoriatic lesions, including the presence of epidermal parakeratosis, acanthosis cell layer thickening, and the downward epidermal extension of in-depth dermis. However, the LTP group (Figure 8c) had a more severe downward epidermal extension of in-depth dermis. Meanwhile, the administration of TwHF (Figure 8d) alleviated the severity of the skin lesion, and the administration of LTP + TwHF (Figure 8e) achieved a similar effect.

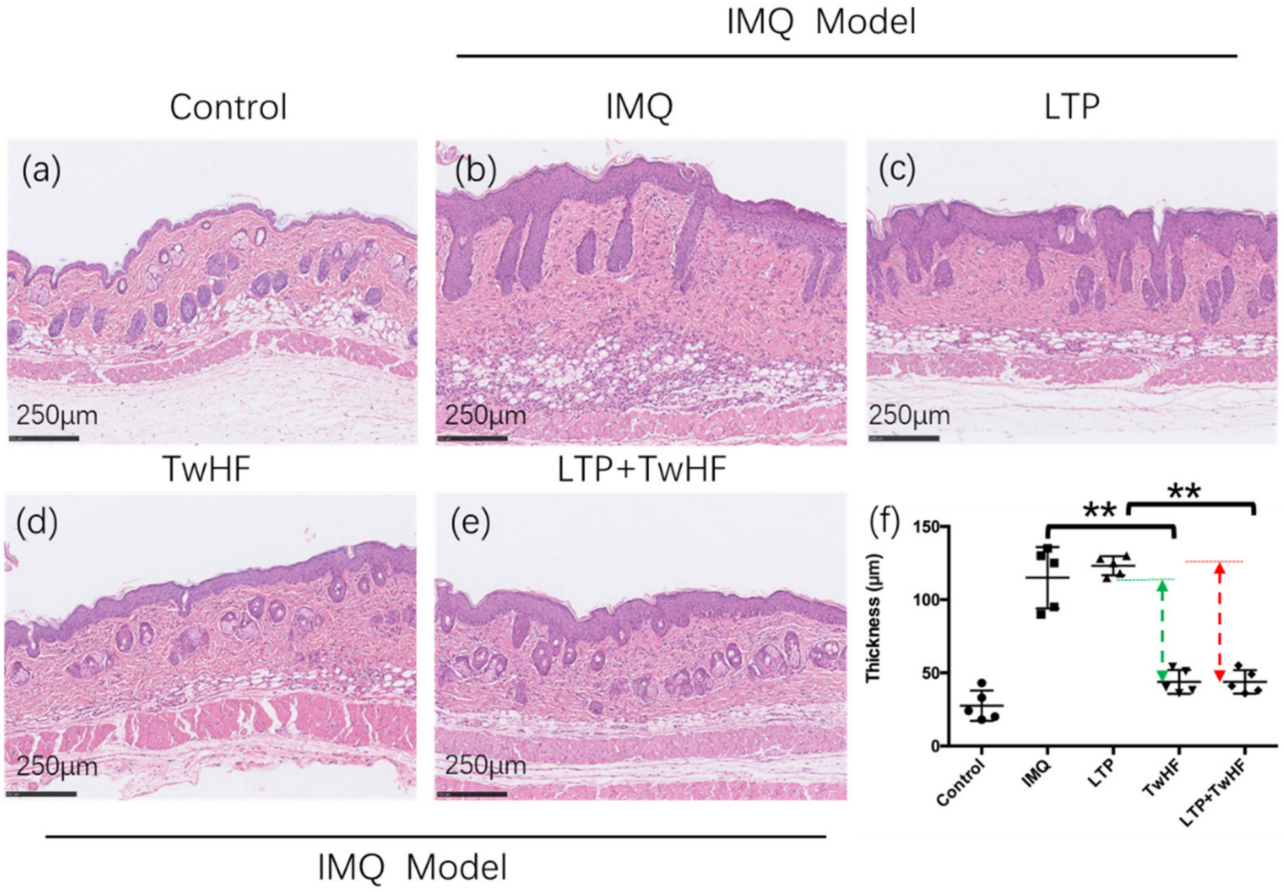

Figure 8. H&E staining of the dorsal skin with the original magnification of 200×. (**a**) Control case, (**b**) IMQ case, (**c**) LTP treatment case, (**d**) TwHF treatment case, (**e**) LTP+TwHF treatment case. (**f**) The thickness of epidermis. Data are expressed as mean ± SD (n = 5 mice/group, ** $p < 0.01$). One representative of three separate experiments is shown while all results were similar among these three experiments. The comparison between the red dash line and the green dash line suggests that the LTP + TwHF psoriasiform dermatitis is more efficient at suppressing epidermal thickening and inhibiting systemic inflammation.

3.3. Plasma + TwHF Treatment Inhibited Inflammatory Cell Infiltration and Inflammatory Cytokines Released in the Skin in the IMQ-Induced Mouse Model

The immunohistochemistry staining of $CD3^+$ T cells was performed to analyze the effect of LTP + TwHF on inflammatory cell accumulation in the skin in the IMQ-induced

mouse model. Figure 9 indicates that the accumulation of T cells in the dermis and epidermis of the LTP group was more than that of the IMQ group. TwHF reduced the abundance of $CD3^+$ T cells in the dermis, and the decrease in the number of positive cells from the LTP group to the LTP + TwHF group was 50% greater than the decrease from the IMQ group to the TwHF group.

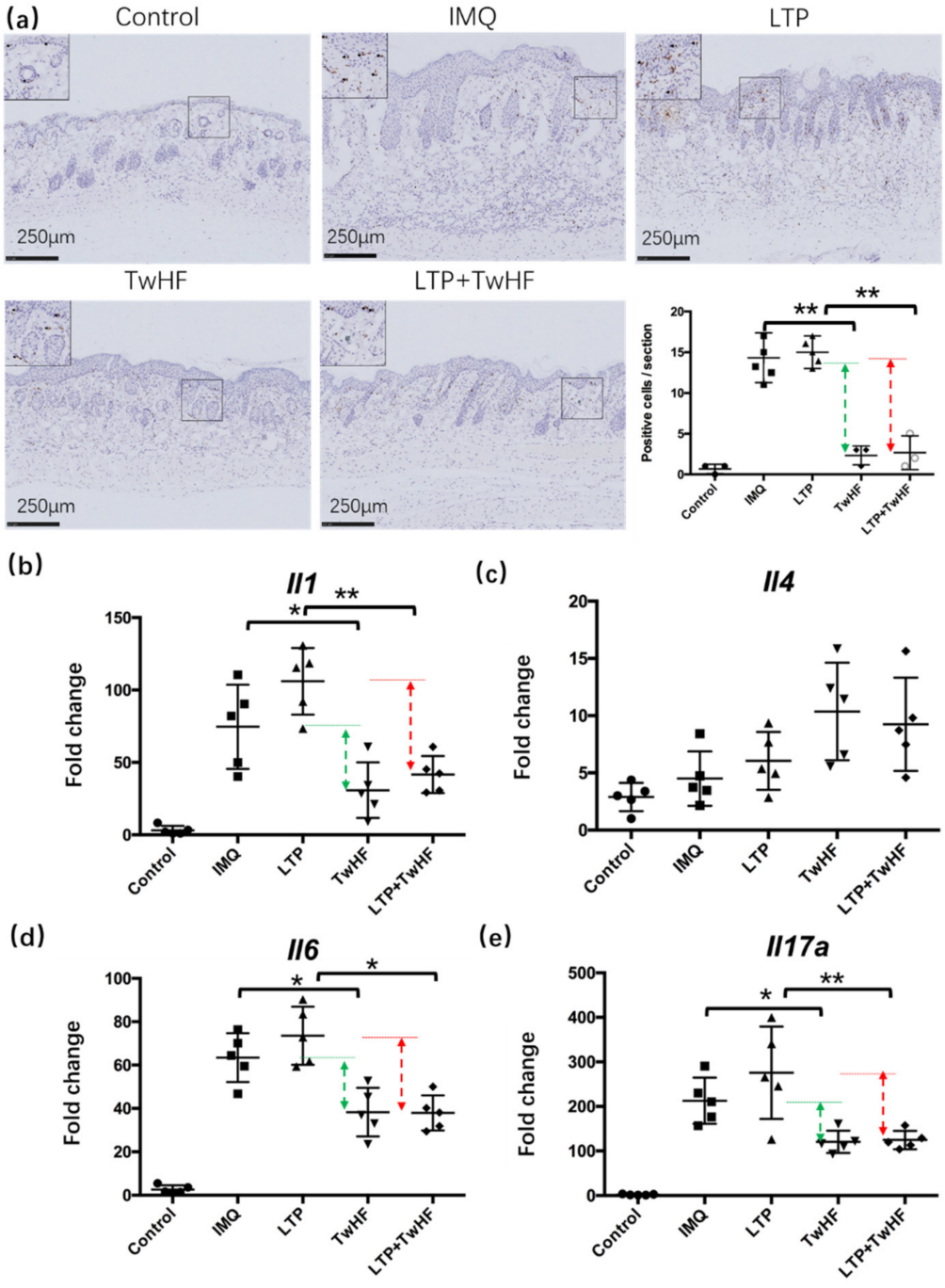

Figure 9. LTP + TwHF treatment inhibited inflammatory cell infiltration and the release of inflammatory cytokines in the skin in the IMQ-induced mice model. (**a**) Immunohistochemical staining of CD3+ cells in skin lesion. (**b**–**e**) The mRNA expression of psoriasis associated with inflammatory cytokines in the skin lesion in the mice model. Data are shown as mean ± SD (**a**–**e**). n = 5 mice. * $p < 0.05$ and ** $p < 0.01$.

The mRNA expression of a set of psoriasis-related inflammatory cytokines in the skin lesions were also tested. Figure 9b–e indicate that the IMQ group have a type 17 cytokine profile (i.e., *Il17a*, *Il6*), without a significant component of type 2 cytokines (i.e., *Il4*) accompanied by the aberrant expression of *Il1* (type 1 cytokines) compared to the control group. The LTP treatment increased these mRNA levels even further. The TwHF treatment decreased the mRNA levels of *Il1*, *Il6*, and *Il17a*, and the decreasing amplitude of these mRNA levels from the LTP group to the LTP + TwHF group was also larger than the decrease in levels from the IMQ group to the TwHF group.

3.4. Plasma + TwHF Treatment Suppressed IMQ-Induced Systemic Inflammation

LTP + TwHF treatment can suppress IMQ-induced systemic inflammation. Figure 10a shows that IMQ increased the relative spleen weight significantly compared to the control group, and that the LTP treatment increased the relative spleen weight even further via the enhanced transdermal delivery of IMQ. LTP + TwHF notably inhibited IMQ-induced splenomegaly. The decrease in the relative spleen weight from the LTP group to the LTP + TwHF group was about 50% more than the decrease from the IMQ group to the TwHF group (Figure 10b). The *Il17a* mRNA levels in the mice's spleen and axillary lymph nodes were also evaluated. Figure 10c suggests that LTP + TwHF inhibited the mRNA levels of *Il17a* in the spleen significantly compared to the LTP group. Meanwhile, the *Il17a* mRNA levels in the axillary lymph nodes only exhibited a little change compared to the control case.

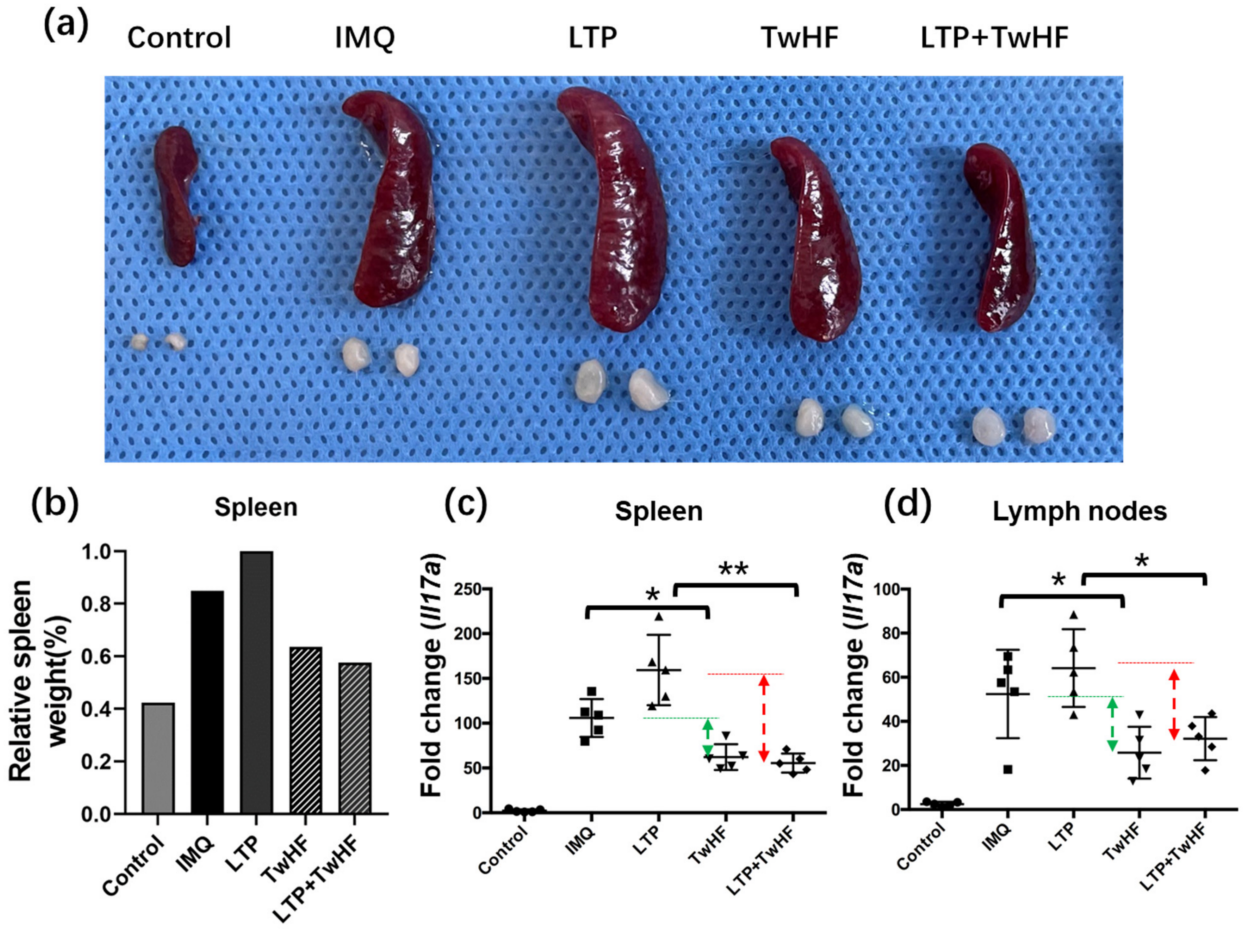

Figure 10. LTP + TwHF suppressed IMQ-induced systemic inflammation. (**a**) Photos of spleen and skin draining lymph nodes taken on the 7th day after IMQ painting. (**b**) Relative weight of spleen of the control and treatment group. The largest spleen of the LTP case is chosen as 100%. (**c**,**d**) The mRNA levels of *Il17a* in the spleen and axillary lymph nodes. (n = 5 mice). * $p < 0.05$ and ** $p < 0.01$.

The TwHF alleviated IMQ-induced psoriasiform dermatitis in mice. Signficiantly, the mice treated with LTP + TwHF showed even lower cumulative scores, epidermal thickening, inflammatory cell infiltration, and inflammatory cytokines released in the IMQ-induced psoriasis-like mouse model. The LTP + TwHF treatment also reduced the enlargement of the spleen efficiently.

4. Conclusions

This study developed a safe, low-cost, and effective LTP jet array for skin disease treatment. This LTP jet array generated a room temperature, active, and large-action-area plasma. The working gas admixture ratio of argon + O_2 (0.1%) produced more RONS, such as O, O_3, and NO, in the plasma plume. The combination of the high concentration RONS and strong electric field of the plasma changed the stratum corneum (the main skin barrier) integrity easily, which meant that plasma could substantially increase the transdermal delivery of medicine. Although the enhanced transdermal delivery of IMQ increased the severity of psoriasiform dermatitis, the improved transdermal delivery of TwHF alleviated this more severe psoriasiform dermatitis. The comparison between TwHF treatment and LTP + TwHF treatment suggests that LTP + TwHF treatment is more efficient at suppressing epidermal thickening and inhibiting systemic inflammation without apparent side effects. LTP + TwHF treatment provides a potential new solution for psoriasis treatment.

Author Contributions: Conceptualization, D.L. and S.Z.; methodology, S.Z.; software, B.C.; validation, B.C.; formal analysis, S.Z.; investigation, S.Z.; resources, H.C.; data curation, B.C.; writing—original draft preparation, D.L.; writing—review and editing, S.Z. and B.C.; visualization, D.L.; supervision, H.C.; project administration, D.L.; funding acquisition, D.L. All authors have read and agreed to the published version of the manuscript.

Funding: This study is supported by the National Natural Science Foundation of China (Grant No. 51777087 and 82173423), the Interdisciplinary Program of Wuhan National High Magnetic Field Center (Grant No. WHMFC202144), Huazhong University of Science and Technology, and Shenzhen Basic Research Project (Natural Science Foundation) (No.JCYJ20190809103805589).

Institutional Review Board Statement: Animal experiments were performed in the Union Hospital, Tongji Medical College, Huazhong University of Science and Technology (USUHS) laboratory animal facility. The protocol used in these experiments was approved by the USUHS Institutional Animal Care and Use Committee (project identification code:20210303-1, approval date: 3rd-March 2021).

Informed Consent Statement: Not applicable.

Data Availability Statement: Some or all data, models, or code generated or used during the study are available from the corresponding author by request (D.L.).

Conflicts of Interest: The authors declare no conflict of interest.

References

1. Gan, L.; Duan, J.; Zhang, S.; Liu, X.; Poorun, D.; Liu, X.; Lu, X.; Duan, X.; Liu, D.; Chen, H. Cold Atmospheric Plasma Ameliorates Imiquimod-Induced Psoriasiform Dermatitis in Mice by Mediating Antiproliferative Effects. *Free Radic. Res.* **2019**, *53*, 269–280. [CrossRef] [PubMed]
2. Gan, L.; Zhang, S.; Poorun, D.; Liu, D.; Lu, X.; He, M.; Duan, X.; Chen, H. Medical Applications of Nonthermal Atmospheric Pressure Plasma in Dermatology. *J. Dtsch. Dermatol. Ges.* **2018**, *16*, 7–13. [CrossRef] [PubMed]
3. Liu, D.; Zhang, Y.; Xu, M.; Chen, H.; Lu, X.; Ostrikov, K. Cold Atmospheric Pressure Plasmas in Dermatology: Sources, Reactive Agents, and Therapeutic Effects. *Plasma Process. Polym.* **2020**, *17*, 1900218. [CrossRef]
4. Griffiths, C.E.; Barker, J.N. Pathogenesis and Clinical Features of Psoriasis. *Lancet* **2007**, *370*, 263–271. [CrossRef]
5. Michalek, I.M.; Loring, B.; John, S.M. A Systematic Review of Worldwide Epidemiology of Psoriasis. *J. Eur. Acad. Dermatol. Venereol.* **2017**, *31*, 205–212. [CrossRef]
6. Ogawa, E.; Sato, Y.; Minagawa, A.; Okuyama, R. Pathogenesis of Psoriasis and Development of Treatment. *J. Dermatol.* **2018**, *45*, 264–272. [CrossRef] [PubMed]
7. Chandra, A.; Ray, A.; Senapati, S.; Chatterjee, R. Genetic and Epigenetic Basis of Psoriasis Pathogenesis. *Mol. Immunol.* **2015**, *64*, 313–323. [CrossRef]

8. Sala, M.; Elaissari, A.; Fessi, H. Advances in Psoriasis Physiopathology and Treatments: Up to Date of Mechanistic Insights and Perspectives of Novel Therapies Based on Innovative Skin Drug Delivery Systems (ISDDS). *J. Control. Release* **2016**, *239*, 182–202. [CrossRef]
9. *Low Temperature Plasma Technology: Methods and Applications*, 1st ed.; Chu, P.K.; Lu, X. (Eds.) CRC Press: Boca Raton, FL, USA, 2013.
10. Lu, X.; Reuter, S.; Laroussi, M.; Liu, D.; Reuter, S.; Laroussi, M.; Liu, D. *Nonequilibrium Atmospheric Pressure Plasma Jets Fundamentals, Diagnostics, and Medical Applications*; CRC Press: Boca Raton, FL, USA, 2019; ISBN 978-0-429-05366-5.
11. Laroussi, M.; Kong, M.G.; Morfill, G.; Stolz, W. *Plasma Medicine: Applications of Low-Temperature Gas Plasmas in Medicine and Biology*; Cambridge University Press: Cambridge, UK, 2012; ISBN 978-1-107-00643-0.
12. Kong, M.G.; Kroesen, G.; Morfill, G.; Nosenko, T.; Shimizu, T.; van Dijk, J.; Zimmermann, J.L. Plasma Medicine: An Introductory Review. *New J. Phys.* **2009**, *11*, 115012. [CrossRef]
13. Heinlin, J.; Morfill, G.; Landthaler, M.; Stolz, W.; Isbary, G.; Zimmermann, J.L.; Shimizu, T.; Karrer, S. Plasma Medicine: Possible Applications in Dermatology. *J. Dtsch. Derm. Ges.* **2010**, *8*, 968–976. [CrossRef]
14. Graves, D.B. Low Temperature Plasma Biomedicine: A Tutorial Review. *Phys. Plasmas* **2014**, *21*, 080901. [CrossRef]
15. Lv, M.; Deng, J.; Tang, N.; Zeng, Y.; Lu, C. Efficacy and Safety of Tripterygium Wilfordii Hook F on Psoriasis Vulgaris: A Systematic Review and Meta-Analysis of Randomized Controlled Trials. *Evid. Based Complement. Altern. Med.* **2018**, *2018*, e2623085. [CrossRef]
16. Wu, C.; Jin, H.-Z.; Shu, D.; Li, F.; He, C.-X.; Qiao, J.; Yu, X.-L.; Zhang, Y.; He, Y.-B.; Liu, T.-J. Efficacy and Safety of Tripterygium Wilfordii Hook F Versus Acitretin in Moderate to Severe Psoriasis Vulgaris: A Randomized Clinical Trial. *Chin. Med. J.* **2015**, *128*, 443–449. [CrossRef]
17. Ru, Y.; Li, H.; Zhang, R.; Luo, Y.; Song, J.; Kuai, L.; Xing, M.; Hong, S.; Sun, X.; Ding, X.; et al. Role of Keratinocytes and Immune Cells in the Anti-Inflammatory Effects of Tripterygium Wilfordii Hook. f. in a Murine Model of Psoriasis. *Phytomedicine* **2020**, *77*, 153299. [CrossRef]
18. Chen, B.; Huang, Z.; Liu, D. Deposition of Charged Aerosols by E × B Enhanced Low-Temperature Plasma Jet Array. *Plasma Process. Polym.* **2021**, *18*, e2100085. [CrossRef]
19. Pei, X.; Liu, J.; Xian, Y.; Lu, X. A Battery-Operated Atmospheric-Pressure Plasma Wand for Biomedical Applications. *J. Phys. D Appl. Phys.* **2014**, *47*, 145204. [CrossRef]
20. Zhang, S.; Zhang, J.; Yu, J.; Chen, X.; Zhang, F.; Wei, W.; Zhang, L.; Chen, W.; Lin, N.; Wu, Y. Hyperforin Ameliorates Imiquimod-Induced Psoriasis-Like Murine Skin Inflammation by Modulating IL-17A–Producing Γδ T Cells. *Front. Immunol.* **2021**, *12*, 635076. [CrossRef]
21. Liu, Z.; Tian, Y.; Niu, G.; Wang, X.; Duan, Y. Direct Oxidative Nitrogen Fixation from Air and H_2O by a Water Falling Film Dielectric Barrier Discharge Reactor at Ambient Pressure and Temperature. *ChemSusChem* **2021**, *14*, 1507–1511. [CrossRef] [PubMed]
22. Gao, H.; Wang, G.; Chen, B.; Zhang, Y.; Liu, D.; Lu, X.; He, G.; Ostrikov, K. Atmospheric-Pressure Non-Equilibrium Plasmas for Effective Abatement of Pathogenic Biological Aerosols. *Plasma Sour. Sci. Technol.* **2021**, *30*, 1507–1511. [CrossRef]
23. Ma, S.; Cheng, H.; Li, J.; Xu, M.; Liu, D.; Ostrikov, K. Large-Scale Ion Generation for Precipitation of Atmospheric Aerosols. *Atmos. Chem. Phys.* **2020**, *20*, 11717–11727. [CrossRef]
24. Yang, Z.; Liu, D. Enhanced Transmembrane Transport of Reactive Oxygen Species by Electroporation Effect of Plasma. *Plasma Process. Polym.* **2021**, *18*, e2100054. [CrossRef]
25. Chen, B.; Liu, D. Mass Spectrometry Study on Ions Generated by Low-Temperature Plasma Jet. *IEEE Trans. Plasma Sci.* **2021**, *49*, 1190–1194. [CrossRef]
26. Zhang, Y.; Cheng, H.; Gao, H.; Liu, D.; Lu, X. On the Charged Aerosols Generated by Atmospheric Pressure Non-Equilibrium Plasma. *High Volt.* **2021**, *6*, 408–425. [CrossRef]
27. Liu, D.W.; Iza, F.; Kong, M.G. Electron Heating in Radio-Frequency Capacitively Coupled Atmospheric-Pressure Plasmas. *Appl. Phys. Lett.* **2008**, *93*, 261503. [CrossRef]
28. Liu, D.W.; Iza, F.; Kong, M.G. Electron Avalanches and Diffused Gamma-Mode in Radio-Frequency Capacitively Coupled Atmospheric-Pressure Microplasmas. *Appl. Phys. Lett.* **2009**, *95*, 031501. [CrossRef]
29. Reuter, S.; Winter, J.; Schmidt-Bleker, A.; Schroeder, D.; Lange, H.; Knake, N.; der Gathen, V.S.; Weltmann, K.-D. Atomic Oxygen in a Cold Argon Plasma Jet: TALIF Spectroscopy in Ambient Air with Modelling and Measurements of Ambient Species Diffusion. *Plasma Sour. Sci. Technol.* **2012**, *21*, 024005. [CrossRef]
30. Liu, X.Y.; Hu, J.T.; Liu, J.H.; Xiong, Z.L.; Liu, D.W.; Lu, X.P.; Shi, J.J. The Discharge Mode Transition and O(5p1) Production Mechanism of Pulsed Radio Frequency Capacitively Coupled Plasma. *Appl. Phys. Lett.* **2012**, *101*, 043705. [CrossRef]
31. Lu, X.; Laroussi, M.; Puech, V. On Atmospheric-Pressure Non-Equilibrium Plasma Jets and Plasma Bullets. *Plasma Sour. Sci. Technol.* **2012**, *21*, 034005. [CrossRef]
32. Marschewski, M.; Hirschberg, J.; Omairi, T.; Höfft, O.; Viöl, W.; Emmert, S.; Maus-Friedrichs, W. Electron Spectroscopic Analysis of the Human Lipid Skin Barrier: Cold Atmospheric Plasma-Induced Changes in Lipid Composition. *Exp. Dermatol.* **2012**, *21*, 921–925. [CrossRef]
33. Maiti, S.; Sen, K.K. *Advanced Technology for Delivering Therapeutics*; BoD–Books: Norderstedt, Germany, 2017; ISBN 978-953-51-3122-9.
34. Liu, X.; Gan, L.; Ma, M.; Zhang, S.; Liu, J.; Chen, H.; Liu, D.; Lu, X. A Comparative Study on the Transdermal Penetration Effect of Gaseous and Aqueous Plasma Reactive Species. *J. Phys. D Appl. Phys.* **2018**, *51*, 075401. [CrossRef]

35. Duan, J.; Ma, M.; Yusupov, M.; Cordeiro, R.M.; Lu, X.; Bogaerts, A. The Penetration of Reactive Oxygen and Nitrogen Species across the Stratum Corneum. *Plasma Process. Polym.* **2020**, *17*, 2000005. [CrossRef]
36. Helmke, A.; Hoffmeister, D.; Mertens, N.; Emmert, S.; Schuette, J.; Vioel, W. The Acidification of Lipid Film Surfaces by Non-Thermal DBD at Atmospheric Pressure in Air. *New J. Phys.* **2009**, *11*, 115025. [CrossRef]
37. Shimizu, K. Biological Effects and Enhancement of Percutaneous Absorption on Skin by Atmospheric Microplasma Irradiation. *PMED* **2015**, *5*, 205–221. [CrossRef]
38. Duan, J.; Gan, L.; Nie, L.; Sun, F.; Lu, X.; He, G. On the Penetration of Reactive Oxygen and Nitrogen Species Generated by a Plasma Jet into and through Mice Skin with/without Stratum Corneum. *Phys. Plasmas* **2019**, *26*, 43504. [CrossRef]
39. Wen, X.; Xin, Y.; Hamblin, M.R.; Jiang, X. Applications of Cold Atmospheric Plasma for Transdermal Drug Delivery: A Review. *Drug Deliv. Transl. Res.* **2021**, *11*, 741–747. [CrossRef]
40. Shimizu, K.; Tran, N.A.; Hayashida, K.; Blajan, M. Comparison of Atmospheric Microplasma and Plasma Jet Irradiation for Increasing of Skin Permeability. *J. Phys. D Appl. Phys.* **2016**, *49*, 315201. [CrossRef]
41. Lee, S.; Choi, J.; Kim, J.; Jang, Y.; Lim, T.H. Atmospheric Pressure Plasma Irradiation Facilitates Transdermal Permeability of Aniline Blue on Porcine Skin and the Cellular Permeability of Keratinocytes with the Production of Nitric Oxide. *Appl. Sci.* **2021**, *11*, 2390. [CrossRef]
42. Zheng, J.R.; Fang, J.L.; Gu, K.X.; Xu, L.F.; Gao, J.W.; Guo, H.Z.; Yu, Y.H.; Sun, H.Z. Screening of active anti-inflammatory-immunosuppressive and antifertile compositions from Tripterygium wilfordii. I. Screening of 8 components from total glucosides of Tripterygium wilfordii (TII). *Zhongguo Yi Xue Ke Xue Yuan Xue Bao* **1987**, *9*, 317–322.
43. Han, R.; Rostami-Yazdi, M.; Gerdes, S.; Mrowietz, U. Triptolide in the Treatment of Psoriasis and Other Immune-Mediated Inflammatory Diseases. *Br. J. Clin. Pharmacol.* **2012**, *74*, 424–436. [CrossRef] [PubMed]